Empirics and models of fragmented lane changes

Mullakkal-Babu, F.A.; Wang, M.; van Arem, B.; Happee, R.

Important note
To cite this publication, please use the final published version (if applicable).
Please check the document version above.

Empirics and Models of Fragmented Lane Changes

FREDDY ANTONY MULLAKKAL-BABU, MENG WANG (Member, IEEE), BART VAN AREM (Senior Member, IEEE), AND RIENDER HAPPEE

Department of Transport and Planning, Faculty of Civil Engineering and Geosciences, Delft University of Technology, 2628 CN Delft, The Netherlands

CORRESPONDING AUTHOR: F. A. MULLAKKAL-BABU (e-mail: freddy.mullakkal_babu.ext@siemens.com)

ABSTRACT Existing microscopic traffic models represent the lane-changing maneuver as a continuous and uninterrupted lateral movement of the vehicle from its original to the target lane. We term this representation as Continuous Lane-Changing (CLC). Recent empirical studies find that not all lane-changing maneuvers are continuous; the lane-changer may pause its lateral movement during the maneuver resulting in a Fragmented Lane-Changing (FLC). We analysed a set of 1064 lane changes from NGSIM dataset which contains 270 FLCs. In comparison to a CLC, this study investigates the distinction of an FLC in terms of its execution and its effects on neighbouring vehicles. We find that during the execution of an FLC, the lane-changer exhibits distinct kinematics and takes a longer duration to complete the lane-changing. We propose a trajectory model to describe the lateral kinematics during an FLC. Additionally, we find that the FLC induces a distinct effect on the follower in the target lane, and propose a model to describe the transient behavior of the target-follower during an FLC. The modelling results suggest that the accuracy of traffic flow models can be improved by deploying lane change execution and impact models that are specific to FLC and CLC. Besides, this study identifies a set of factors that might be related to the decision-making process behind FLC: an average driver executes an FLC when the preceding and following vehicles in the target lane are slower, and when the follower in the target lane is closer than those observed during the onset of a CLC. Our findings suggest that FLC is motivated by an increased necessity to change lane such as during a mandatory lane change.

INDEX TERMS Lane-changing trajectory, fragmented lane change, lane-changing execution.

I. INTRODUCTION

LANE-CHANGING maneuvers have profound impacts on the traffic flow [1] and therefore receive extensive research attention. In order to change-the-lane, the driver must perform at least two tasks: 1) decide if and when to initiate the maneuver; 2) operate the steering and acceleration to execute the maneuver. We refer to the first task as lane-changing decision and the second task as lane-changing execution. The process of lane-changing may also be depicted in more than two steps [2], [3]. Besides, lane-changing impacts other vehicles in the vicinity, which we refer to as lane-changing impact. Therefore a complete description of lane-changing (LC) entails models for its decision, execution and impact.

The review of this article was arranged by Associate Editor Abdulla Hussein Al-Kaff.

Existing studies primarily focus on the LC decision and the impact [1], [4], [5]. The LC decision is typically modelled based on two considerations: the driver's preference for the target lane; and assessment of the safety of the available target gap. Accordingly, LC decision models typically consist of a lane preference model and a complementary gap acceptance model [6], [7], [8], [9], [10]. On the other hand, LC impact models capture the impacts induced by lane changes. The impacts refer to the macroscopic traffic flow characteristics and microscopic behaviors induced by lane changes. At the macroscopic level, lane changes have a direct influence on phenomena such as traffic breakdowns [11] and traffic stop-and-go oscillations [12], and might destabilise the traffic flow [13]. At the microscopic level, an LC temporarily changes the longitudinal behavior of the lane-changer and its surrounding vehicles. Several

studies report a process known as relaxation by which the target-follower accepts short-spacing to facilitate the lane change and relaxes to equilibrium spacing after the lane change [14], [15], [16]. Zheng *et al.* [16] identified another process known as anticipation by which the target-follower's longitudinal behavior changes upon noticing the lane change intention.

Compared to LC decision and impact, studies on lane change execution are rare. Existing studies on LC execution indicate that the human driver uses visual feedback to adjust the steering-control actions [17]. Salvucci and Gray [18] modelled steering-control as a closed-loop process. The above-mentioned studies are performed in a driving simulator, which provides detailed measurements to analyze the steering-wheel angle and the brake pedal position during the LC execution. However, the artificial setting in a driving simulator is different from the on-road driving environment and might detriment the transferability of the findings. Alternatively, researchers analyzed LC execution as observed from the LC trajectory. The trajectory samples can be extracted from road-side traffic observations. Li *et al.* [19] derived the steering pattern of the lane changes from trajectory samples. Toledo and Zohar [20] analyzed and modelled the LC duration. Wang *et al.* [21] implemented a heuristic-based approach to filter out abnormal trajectories and to define the start and end of an LC trajectory. They identified that a normal LC can be approximately depicted by fifth-degree polynomials. Similarly, several researchers have modelled the lane-changing trajectories [22], [23], [24], [25]. Recently, Yang *et al.* [24] observed two types of lateral movement during LC. We term them as Continuous lane-changing (CLC) and Fragmented lane-changing (FLC). During CLC, the vehicle uninterruptedly moves to the target lane; whereas, during FLC, it exhibits a temporary pause in the lateral movement before the completion of LC. Apart from the apparent difference in lateral movement, so far, it is not clear if FLC trajectories represent a distinct type of lane-changing.

Fragmented lane changes present a methodological challenge to current behavioral-models, which rely on a normative representation of LC. The current models describe the LC decision as a choice between changing the lane and remaining in the current lane, treating lane change execution as an open-loop process. But the driving-simulator-based studies suggest that LC execution is a closed-loop process [17] and the driver might revise the LC decision during the execution: for instance the driver might abort a pre-initiated lane change for safety reasons. The current LC impact models represent the duration of LC as a fixed value; typically the mean or mode of observed sample distribution [26]. The use of summary statistics is only reasonable to represent unimodal distributions, i.e., if all the data points come from a single type of lane-changing. Furthermore, the fixed lane change duration might not be representative of FLC, considering the findings by Yang *et al.* [24] that FLC's are longer than CLC's.
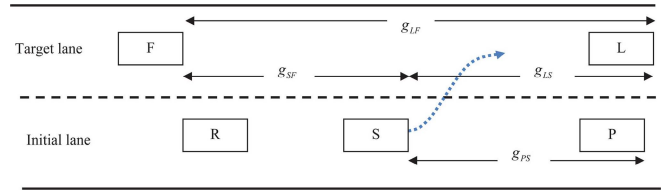

FIGURE 1. Illustration of the influential neighbouring vehicles during a typical lane change manoeuvre.

Fragmented lane changing was ignored in traffic studies so far as its unique impact on traffic flow remained unknown. As a first step towards addressing this knowledge gap, we establish the distinct properties of FLC execution and impact, identify the factors that are associated with FLC, and propose models to describe the lateral kinematics and the microscopic impact induced by FLC on the target-follower. Our results highlight the relevance of this maneuver in traffic studies.

II. DATA EXTRACTION AND CLASSIFICATION OF TRAJECTORY SAMPLES

This section describes the dataset and the algorithm to extract and classify the LC trajectory samples. This study uses trajectory dataset collected by the FHWA's Next Generation Simulation (NGSIM) program. Several researchers have previously used this dataset to analyze and model the lane-changing behavior [16], [24], [26]. The vehicle trajectories were extracted from the video images of northbound traffic on I-80 in Emeryville, California. The study site is approximately 500 m long. The vehicle positions were recorded every 0.1s from 4.00 p.m. to 4.15 p.m. and from 5:00 p.m. to 5:30 p.m. on April 13, 2005.

In order to identify and classify the observed lane-changing maneuvers, the vehicle trajectories logged in the NGSIM dataset have to be processed. Towards this, we develop a systematic method which is presented in Algorithm 1. Figure 1 illustrates the vehicles involved in the lane change: *F* (follower in the target lane), *L* (leader in the target lane), *P* (preceding vehicle in the initial lane), and *R* (follower in the initial lane).

Algorithm 1 consists of two major loops. The first loop identifies the LC instances and corresponding insertion time t_{LC} from the NGSIM dataset. Here, t_{LC} denotes the insertion point, i.e., the time instant at which centre of the vehicle's front edge crosses the lane boundary marking. This approach is similar to previous studies [16], [24]. Secondly, it filters out LC instances in which the subject vehicle's trajectories are not observable for at least a $T \in [t_{LC} - 7, t_{LC} + 7]$. The time interval of 14 s was found to be long enough to entirely cover all lane change executions [10]. Thereafter, it logs the trajectories of the subject and neighbouring vehicles, for the selected LC instances.

The second loop of Algorithm 1 identifies the start and end of the lane change. The lane-changer's trajectory between the start and the end of the lateral displacement (larger than a threshold) is typically identified as the CLC trajectory [10].
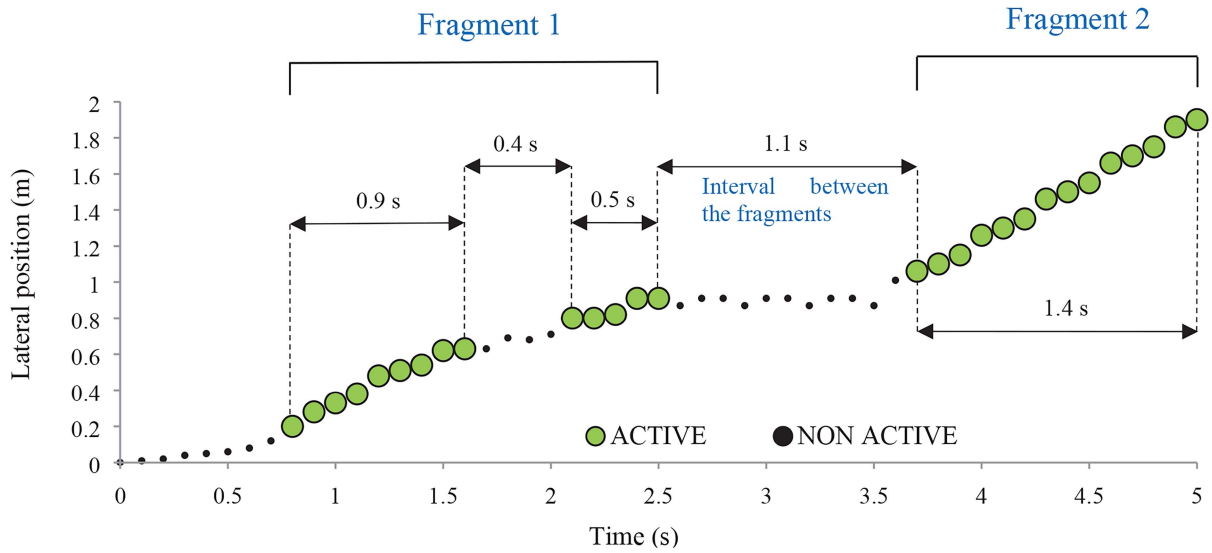
FIGURE 2. Illustration of the method to identify the LC fragments.

In the case of an FLC, a marginal lateral movement might only indicate an intermediate pause and does not necessarily mean that the LC is complete. The procedure to determine the LC duration is illustrated in Figure 2. First, it identifies all the time instances when the subject vehicle's average lateral displacement is larger than a threshold. An averaging interval shorter than 0.3 s yields indiscriminately large number of time points within T and longer interval detriments the accuracy of temporal bounds. Moreover, the threshold should discriminate between the lateral activity exhibited during active lane-changing and that during lane-keeping or an intermediate pause. Accordingly, a vehicle is identified as laterally active, i.e., $d^*(t) = 1$, if it exhibits an average lateral displacement larger than 0.1 m over the previous 0.3 s, where $d^*(t)$ is defined as

$$d^*(t) = \begin{cases} 1 & if \ |y(t) - y(t-0.3)| \geq 0.1 \\ 0 & if \ |y(t) - y(t-0.3)| < 0.1 \end{cases} \quad (1)$$

where y denotes the global lateral coordinate of the vehicle's front-centre. The second step is to identify one or more series of lateral active points that represents continuous lateral movement or LC fragment. An LC fragment is defined as a sequence of at least 5 laterally active points; or a combination of such sequences that are separated by an interval of not more than 1 s. Here, 1 s threshold implies that during the interval between the fragments the vehicle did not move more than 0.33 m laterally, i.e., approximately 0.15 times the vehicle width.

Algorithm 1 classifies the LC trajectories based on the number of fragments. The lane change trajectory with a single fragment is classified as Continuous Lane Change trajectory, and that with two fragments is classified as Fragmented Lane Change trajectory. Finally, Algorithm 1 determines the temporal bounds of LC's. The timestamp of the first active-point of the first fragment is labelled as t^{start} denoting the lane change start point, and the timestamp of
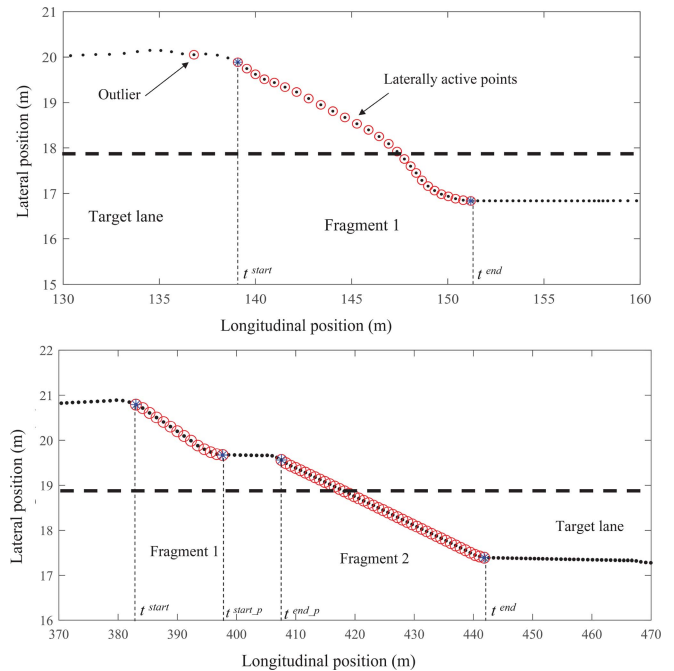
FIGURE 3. Illustration of extraction and classification of observed lane-changing trajectories: (a) an observed CLC trajectory and (b) an observed FLC trajectory. The black dots depict the observed positions; the red circles represent the laterally active points, and the blue asterisk depicts the critical moments along during the lane change, the dashed line represents the lane boundary.

the last active point of the last fragment is labelled as t^{end} denoting lane change endpoint. The interval between t^{start} and t^{end} is labelled as D denoting the lane change duration. In case of an FLC, the timestamp of last active point of the first fragment is labelled as t^{start_p} denoting the start of the intermediate pause and the timestamp of the first active-point of the second fragment is labelled as t^{end_p} denoting the end of the intermediate pause. Figure 3 shows example trajectories of an FLC and a CLC as extracted by the algorithm.

Algorithm 1 Pseudo Algorithm to Extract and Classify the Lane-Changing Trajectories in NGSIM Dataset

1: **Data**: NGSIM trajectory data log consisting of the following elements: row number (k), observation time (t), vehicle ID, x coordinate, y coordinate, lane number, preceding vehicle ID, rear vehicle ID

2: **Result**:Trajectory of the subject vehicle S and neighbouring vehicles F,R,L,P during lane-changing

3: **Result**:Critical time points of the lane change trajectory: t_{LC}, t_{start},t_{end}, t_{start_p},t_{end_p}

4: **while** $k < length(datalog)$ **do**

5:     **if** vehicle ID (k) = vehicle ID($k + 1$)) AND lane number (k) $\neq$ lane number ($k + 1$) **then**

6:         **begin**

7:         lane change instance LC (i) = k; $t_{LC} = t(k)$

8:         **if** trajectory of S available for T **then**

9:             **begin**

10:             $R \leftarrow$ rear vehicle ID (k), $P \leftarrow$ preceding vehicle ID (k)

11:             $F \leftarrow$ rear vehicle ID ($k+1$), $L \leftarrow$ preceding vehicle ID ($k + 1$)

12:             Neighbours (i) $\leftarrow S, R, P, F, L$ during T

13:             $i = i + 1$

14:             **end**

15:         **end**

16: **while** $j < length(LC)$ **do**

17:     **begin**

18:     Calculate $d^*(t)$ of S and identify the laterally active points based on Eq. (1)

19:     Apply rules to identify fragments

20:     **if** number of fragment = 1 **then**

21:         LC type(i) $\leftarrow$ CLC

22:     **if** number of fragment = 2 **then**

23:         LC type(i) $\leftarrow$ FLC

24:     **else**

25:         remove

26:     Identify t_{start}, t_{end}, t_{start_p}, t_{end_p}

27:     **end**

Lane change samples extracted by the algorithm were filtered before further analysis. To avoid non-typical trajectories, lane changes by heavy vehicles or those in which the lane-changer made two or more subsequent lane changes were excluded. We found that the lateral coordinates of certain locations (probably at the junction of the frame's boundaries of NGSIM recording cameras) are skewed. The lane changes at these locations were omitted. Accordingly, we obtained 794 CLC and 270 FLC samples. The velocity and acceleration were estimated from the vehicle positions every 0.1 s. In the analysis, we will use the extremes of these variables such as maximum lateral velocity and maximum lateral acceleration. However, extremes are directly affected by the noise in the dataset. In order to avoid such extremes, we smoothened these variables by employing a double-sided moving average filter proposed by [27]. The

velocity was smoothened with a time window of 1 s, and the acceleration with a time window of 2 s. The smoothening procedure and time span were chosen based on the recommendations in [28].

As the first step, we test the assumption of unimodality of LC duration samples. This assumption forms the basis of normative representation of LC in the existing behavioral studies. The dip test result reveals that the lane change duration distribution exhibits a strong bimodality: $p = 0.005 < 0.01$; Hartigan's dip = 0.0185. The bimodality suggests that the sampled lane change trajectories are not the outcome of more than one process. Additionally, this finding strengthens the motivation to investigate if FLC represents a distinct type of lane changing.

III. COMPARATIVE ANALYSIS AND MODELS OF LC EXECUTION

This section compares the lane change execution of FLC's and CLC's. Towards this, we first perform a comparative analysis of LC execution as observed from the two types of LC trajectories. Thereafter, we present a model of lateral kinematics during FLC execution.

A. COMPARISION OF KINEMATICS DURING LANE-CHANGING

Lane change execution consists of acceleration and steering operation. The steering operation during a typical CLC can be distinguished into two sequential phases of steering sub-movements as shown in Figure 4. This analysis approach has been used in previous studies [17]. During the first phase, the steering wheel is turned to a maximum angle; and during the second phase, the steering wheel turns in the opposite direction. The second phase ends when the steering wheel angle reaches a second peak. Since this steering operation cannot be directly observed in the trajectory dataset, we define observable kinematic variables based on the above description of steering execution. The first and second steering angle peaks induce extremes in lateral acceleration due to the dynamics of vehicle movement as shown in Figure 4. The maximum triggering acceleration $a_{y,S}^t$ denotes the absolute maximum lateral acceleration in the first steering phase, and maximum stabilizing acceleration $a_{y,S}^s$ denotes the absolute maximum lateral acceleration in the second phase. We choose the absolute value of acceleration as it allows to jointly analysing the left and right lane change trajectories. The peak in the heading angle is accompanied by the maximum lateral velocity $v_{y,S}^{max}$ [29]. The acceleration operation during LC execution is analyzed in terms of $a_{x,S}^{avg}$ denoting the average longitudinal acceleration. To summarise, we analyze LC execution using the following set of kinematic variables: D, $v_{y,S}^{max}$, $a_{y,S}^t$ and $a_{y,S}^s$.

To compare the FLC and CLC executions, we test the null hypothesis that the mean of kinematic variables observed is equal between the two LC types, with two-tailed independent sample t-test. We reject the null hypothesis if the p-value is less than the significance level of 0.05. The test
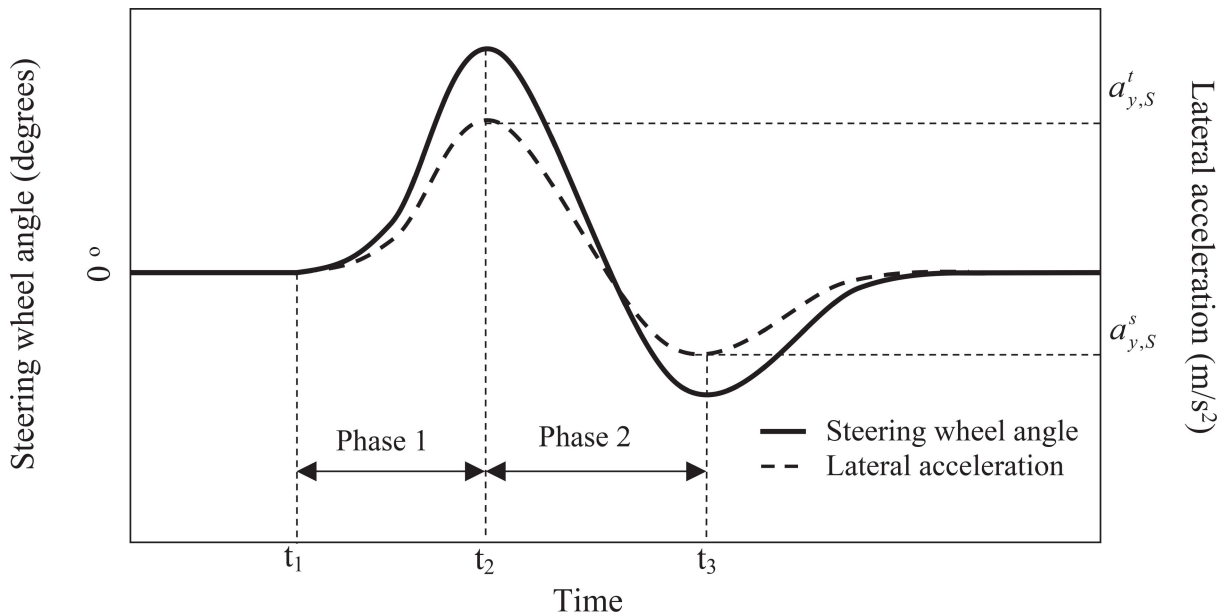
FIGURE 4. Illustration of steering sequence for CLC adapted from [30].

TABLE 1. Comparative analysis of trajectory kinematics.

Parameter	LC TYPE (sample size)	Mean (Std. Error)	Difference (Std. Error)	t	Sig (2-tailed)
Average forward acceleration (m/s^2)	CLC (794)	0.05 (0.02)	0.09	2.58	0.01
	FLC (270)	-0.03 (0.02)	-0.03		
Maximum triggering acceleration (m/s^2)	CLC (794)	1.13 (0.03)	0.19	3.36	<0.001
	FLC (270)	0.94 (0.04)	-0.05		
Maximum stabilising acceleration (m/s^2)	CLC (794)	-0.53 (0.02)	0.06	1.33	0.181
	FLC (270)	-0.60 (0.03)	-0.05		
Maximum lateral velocity (m/s)	CLC (794)	1.02 (0.01)	0.04	1.87	0.062
	FLC (270)	0.98 (0.01)	-0.02		
Lane change duration (s)	CLC (794)	4.67 (0.07)	-3.23	-22.3	<0.001
	FLC (270)	7.91 (0.13)	-0.14		

results presented in Table 1 suggest that LC execution of the FLC is different from a CLC. On average, the FLC spans a duration of 7.91 s, which is significantly longer than that of CLC 4.67 s as shown in Figure 5. This might be a possible reason for the bimodality of LC duration samples reported in Section II. The vehicles performing CLC accelerates (0.05 m/s^2) more compared to FLC (−0.03 m/s^2). The larger longitudinal acceleration observed during a CLC might be related to the lane-changer's attempt to adapt to higher velocity in the target lane. However, this hypothesis will be tested in the next section. For both types of LC's, the maximum triggering acceleration is significantly larger than the maximum stabilising acceleration. Such an asymmetry might be due to the underlying steering profile [30]. The first peak in steering angle (corresponding to $a_{y,S}^s$) is typically higher than that of the second peak (corresponding to $a_{y,S}^s$). Salvucci and Gray [18] attribute this asymmetry to the closed-loop steering process based on visual feedback. More precisely, the human driver controls the steering during the

LC based on updated visual information on vehicle course and the target road region. Between the two types of LC's, a vehicle performing CLC is observed to have larger maximum triggering acceleration $a_{y,S}^s$ than an FLC; whereas maximum stabilising acceleration $a_{y,S}^s$ does not differ significantly. A possible explanation is that the driver's preparation for the lane change is primarily reflected in the first steering phase. The second phase consists of steering movement based on visual feedback to stabilise the vehicle on the trajectory [30]. To summarise, the results confirm that the fragmented and continuous lane change trajectories are outcomes to two distinct processes of LC execution and agree with the existing notion that LC execution is a closed-loop process.

B. MODELS OF LATERAL KINEMATICS DURING LC EXECUTION

In this section, we propose a model of lateral kinematics along FLC trajectory and evaluate its fit with the observed trajectories. The functional form of the model should meet
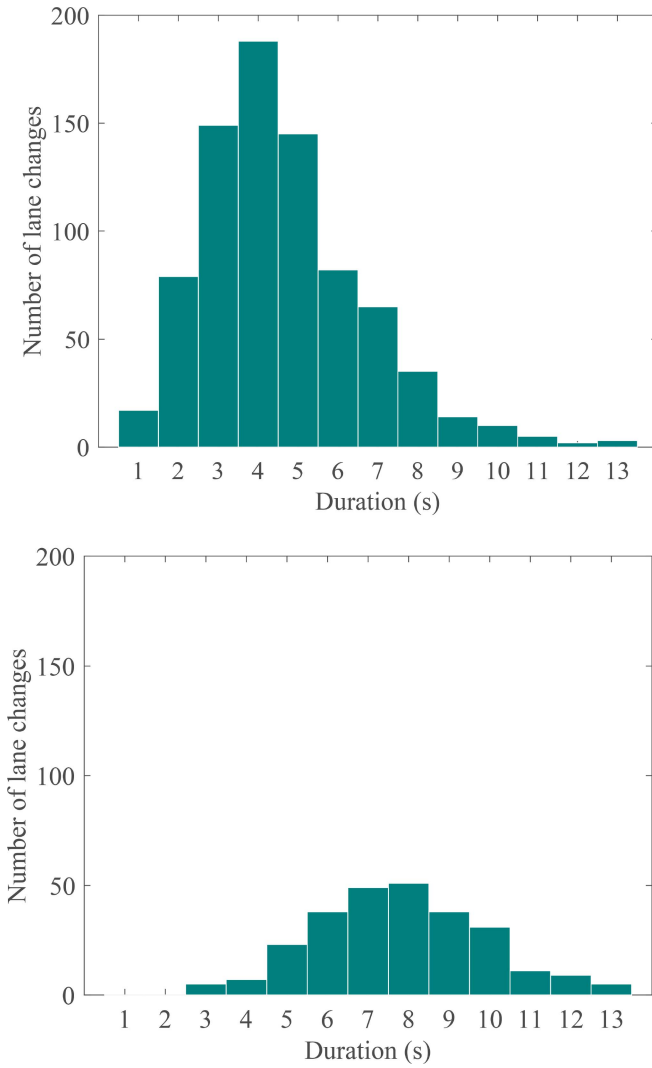
FIGURE 5. Frequency distribution of duration: a) continuous lane-changing b) fragmented lane-changing.

two requirements. First, the functional form should be differentiable at least until the second order. This is to ensure that the velocity and acceleration variables can be derived from the model. Secondly, the functional form should allow the distinctive lateral kinematic constraints of the FLC trajectory: 1) the vehicle laterally moves from the centerline of original to that of target lane during LC, i.e., $|y(t^{start}) - y(t^{end})| = W$; 2)the vehicle does not move laterally at the onset and end of LC, i.e., $v_y(t^{start}) = v_y(t^{end}) = 0$; $a_y(t^{start}) = a_y(t^{end}) = 0$ and 3) the vehicle does not move laterally during the pause between the two LC fragments, i.e., $v_y(t) = a_y(t) = 0 : t \in [t^{start\_p}, t^{end\_p}]$ where W denotes the total lateral displacement during a lane change.

Existing literature contains several models to describe an LC trajectory. The simplest and prominent representation of LC trajectory is the Linear Trajectory Model (LTM) described as follows:

$$y(t) = y(t_0) + \frac{W}{D}(t - t^{start}) \qquad (2)$$

However, the LTM implicitly assumes constant lateral velocity and cannot represent the variation in acceleration. Therefore, this model does not meet the first functional requirement. Several other functional forms overcome this limitation such as polynomial models [21]; trapezoidal acceleration model [31]; linear acceleration model [24]; hyperbolic tangent model [32] and the Sinusoidal lateral Acceleration Model (SAM). Since empirical studies on human lane change trajectory show that lateral acceleration profiles during LC can be represented as a sinusoidal function [33], we select the SAM for further evaluation. This model has been widely used to describe the LC trajectory [33], [34], [35]. The SAM expresses the lateral position during LC (the second derivative of the lateral acceleration) as:

$$y(t) = y(t^{start}) + \frac{-W}{2\pi} \sin\left(\frac{2\pi (t - t^{start})}{D}\right)$$

$$+ \frac{W(t - t^{start})}{D} \qquad (3)$$

However, SAM does not meet the second functional criteria. Therefore, we propose a new model: Double Sinusoidal lateral Acceleration Model (DSAM). Among the FLC samples, the mean (standard error) duration of the first fragment is 2.58 s (0.9 s) and that of the second fragment is 2.69 s (0.1 s). This suggests that the average duration of the two fragments were approximately equal. Similarly, during the pause between the fragments the lane-changer is close to the lane marking; with a mean (standard error) lateral position error of 0.15 m (0.7 m). Based on these findings, this model assumes that a vehicle moving along an FLC trajectory achieve the total lateral displacement in two equal phases. Accordingly, the trajectory consists of two equal cycles of lateral sinusoidal accelerations, separated by a brief pause as illustrated in Figure 6. The DSAM can be expressed in terms of the lateral position as:

$$y(t) = \begin{cases} y(t^{start}) + \frac{-W}{4\pi} \sin\left(\frac{2\pi (t-t^{start})}{d}\right) + \frac{W(t-t^{start})}{2d}; \\ \quad if : t^{start} < t \le t^{start} + d \\ y(t^{start}) + \frac{W}{2}; \\ \quad if : t^{start} + d < t \le t^{start} + d + t_w \\ y(t^{start}) + d + \frac{-W}{4\pi} \sin\left(\frac{2\pi (t-t^{start}-d-t_w)}{d}\right) + \\ \quad \frac{W(t-t^{start}-d-t_w)}{2d}; \\ \quad if : t^{start} + d + t_w < t \le t^{start} + 2d + t_w \end{cases} \qquad (4)$$

where $t_w = t^{end\_p} - t^{start\_p}$ denotes the duration of the intermediate pause in seconds, $d = \frac{D-t_w}{2}$ denotes the duration of each lateral acceleration cycle.

C. PERFORMANCE EVALUATION

We evaluate the performance of the DSAM model in representing the lateral kinematics of observed FLC trajectories and compare it with LTM and SAM (a more reasonable approximation of CLC). The model parameters: D, W, t_w were estimated for each sampled observation of lane-changing trajectory by Algorithm 1 as illustrated in Figure 2.
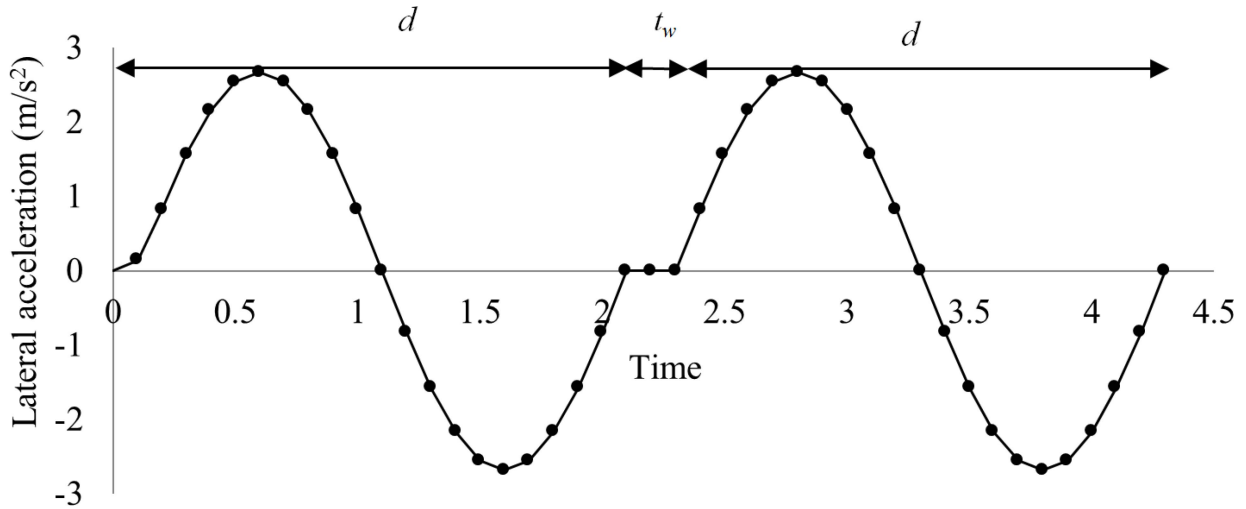
FIGURE 6. Illustration of the double sinusoidal lateral acceleration model for a fragmented lane change.

TABLE 2. Summay of performance evaluation of the LC trajectory models.

LC Type	Trajectory model	MAE values [% error reduction *w.r.t.* LTM]			
		y in m	$v_{y,S}^{max}$ in m/s	$a_{y,S}^{t}$ in m/s^2	$a_{y,S}^{s}$ in m/s^2
FLC	LTM	0.36	0.6	N.A	N.A
	SAM	0.42 [-17 %]	0.25 [57 %]	0.42	0.54
	DSAM	0.35 [2 %]	0.22 [62 %]	0.34	0.42
CLC	LTM	0.27	0.51	N.A	N.A
	SAM	0.21 [20 %]	0.23 [55 %]	0.54	0.48

To match the observed trajectory sampling interval, the lateral positions of the vehicle were modelled at an interval of 0.1 s. The lateral velocity and lateral acceleration of the artificial trajectories were numerically estimated from simulated vehicle positions every 0.1 s. Figure 7 shows examples of modelled and observed LC trajectories. We evaluate the modelling accuracy of four variables: y, $v_{y,S}^{max}$, $a_{y,S}^{t}$ and $a_{y,S}^{s}$. As shown in Table 1, these variables reflect the distinction in the FLC trajectory. The performance of the three models was compared in terms of the Mean Absolute Error (MAE) = $\frac{1}{N} \sum_{1}^{N} |X_{observed} - X_{simulated}|$. Here, N denotes the total number of trajectory samples. The MAE values in Table 2 indicate that trajectories produced by the DSAM describe the observed FLC trajectories more accurately than the SAM and LTM. Interestingly, the simple LTM is able to describe lateral positions during FLC with a comparable level of accuracy and is even better than the SAM model. However, DSAM provides a significant increase in the estimation accuracy of $v_{y,S}^{max}$, $a_{y,S}^{t}$ and $a_{y,S}^{s}$ and therefore can be regarded as the best approximation of FLC trajectory. The results suggest that SAM indeed provides a better representation of a CLC trajectory than LTM.

IV. COMPARATIVE ANALYSIS AND MODELS OF LC IMPACT
This section compares the microscopic impacts induced by FLC's and CLC's. First, we analyze the change in kinematic states of ambient vehicles during each type of LC. Towards this, we compare the relative kinematic state of neighbouring vehicles at the onset and at the end of the lane change. Secondly, we propose models to describe the effect of each type of lane change on the behavior of the target-follower.

A. RELATIVE KINEMATICS OF AMBIENT VEHICLES AT THE ONSET OF LANE CHANGE
As depicted in Figure 1, the lane change by S is influenced by neighbouring vehicles *F*, *L* and *P*. We use the space headway and relative velocity as explanatory variables (EV) to characterise the relative kinematics of neighbouring vehicles. This set of variables has been used in previous studies to explain the LC decision [2], [4], [22]. For each LC, the values of explanatory variables were calculated at $t - 0.2, t - 0.1, t, t + 0.1, t + 0.2$, and the average value during instances was used as the representative value in this study. The approach reduces the error caused by instantaneous measurements in NGSIM data [36]. To examine the traffic conditions at the onset of the two LC types, we compare the distribution of their EV. Towards this, we test the null hypothesis, $H_0 : \mu_{EV\_CLC}(t^{start}) = \mu_{EV\_FLC}(t^{start})$, i.e., the mean EV of the two LC types are equal. Here, $EV \in \{g_{SF}, g_{LS}, g_{PS}, g_{PF}, \Delta v_{SF}, \Delta v_{LS}, \Delta v_{PS}, \Delta v_{PF}\}$. g_{ij} denotes the space headway of i w.r.t j and is calculated as $v_i - v_j$. Additionally, incomplete vehicle trajectories were filtered out from the analysis.
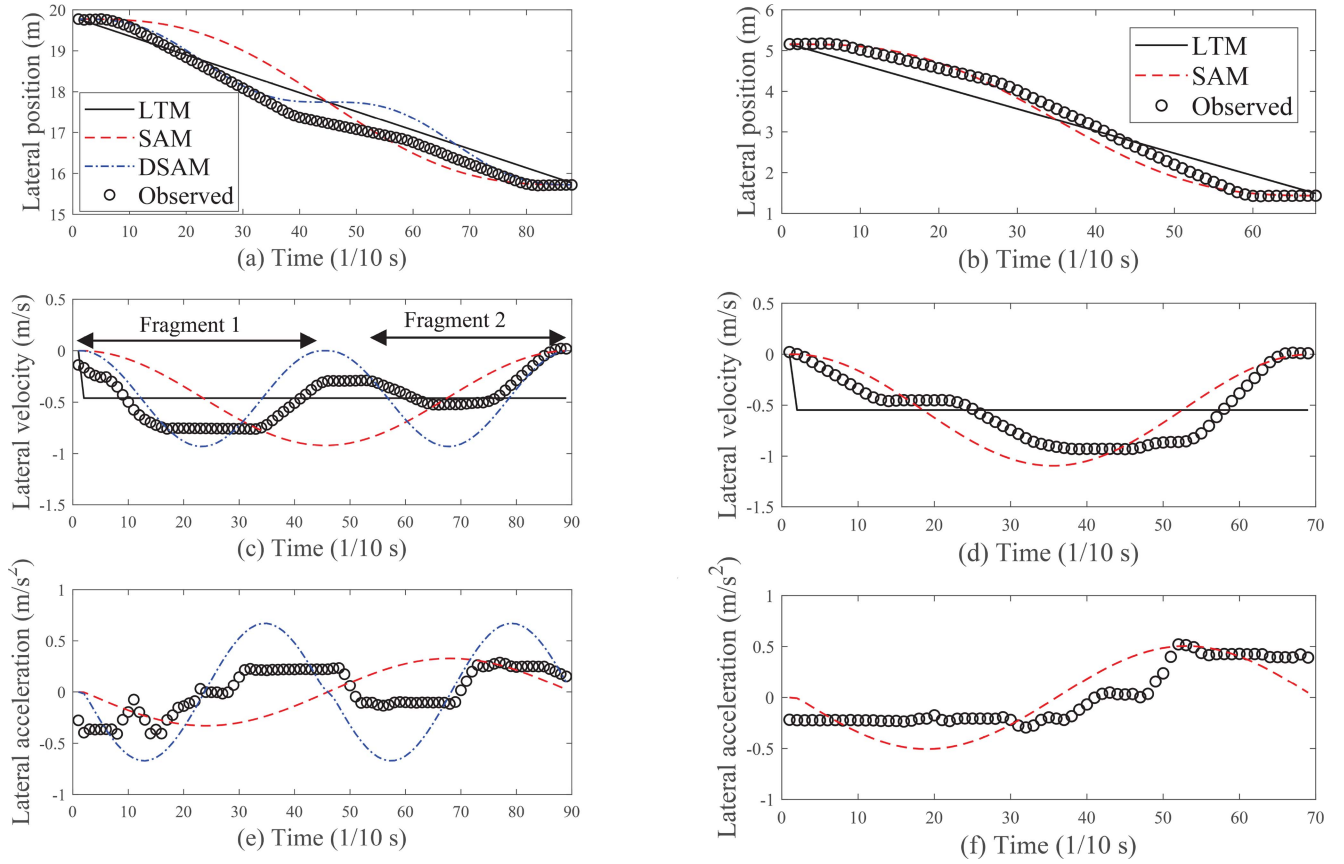
FIGURE 7. Example of simulated and observed lane-changing trajectories of FLC (a, c, e) and CLC (b, d, f).

Table 3 summarises the test results. We reject the null hypothesis if the p value is less than the significance level of 0.05. It can be seen that the mean g_{SF} and g_{PS} are significantly different between the two LC types: in comparison to CLC, the FLC emerges when lane-changer is closer to F; and farther away from P. Both these observations can be explained intuitively: the lower g_{SF} prevents the driver from quickly entering the target lane, and the higher g_{PS} allows the driver to remain longer in the original lane and to complete the LC relatively slower. Secondly, the mean Δv_{SF} and Δv_{LS} are significantly different between the two LC types: the FLC emerged when lane-changer is at higher velocity (on average) relative to F and L; whereas a CLC emerged when the lane-changer is at a lower velocity (on average) relative to F and L. Assuming that the initial conditions of CLC as the standard, an average driver exhibits a preference for FLC when confronted with the relatively slower vehicles on the target lane including a closer follower, and a distant preceding vehicle. These results reveal the distinct traffic conditions related to the emergence of FLC. Additionally, the results in Table 3 shed light on the determinants of the choice of LC type. The EV's, underlying most of the LC decision models, are computed at the lane change insertion (t_{LC}). On the contrary, EV's listed in the present study are observed at the start of the LC. This approach is appropriate to analyze the determinants of FLC decision-making. First,

EV's observed at t_{LC} is influenced by the anticipation behavior following vehicles, and might not represent the relative kinematic state that the driver considers during the decision-making. Secondly, the choice of the FLC is made prior to lane change execution as it requires a pre-calculated steering profile. Therefore, EV observed at the start of the lane maneuver: t_{LC}^{start} could describe the decision-making process more accurately.

B. CHANGE IN THE RELATIVE KINEMATICS BY THE END OF LANE CHANGE

In order to evaluate the impact induced by the lane change, we compare the change in relative kinematics during each of the LC types. More precisely, we compare the change in the mean EV between the start and end of the LC, denoted as $\Delta EV = EV(t^{end}) - EV(t^{start}) : EV \in \{g_{SF}, g_{LS}, \Delta v_{SF}, \Delta v_{LS}\}$. Towards this, we test the null hypothesis, $H_0 : \mu_{\Delta EV\_CLC} = \mu_{\Delta EV\_FLC}$, and the results are summarised in Table 4. To interpret the change, we use the ambient traffic state at the start of LC (Table 3) as the reference. Certain variables exhibited significantly different transitions. First, the mean transition of g_{SF} is significantly different. An average vehicle performing FLC gained a larger headway with F ($\Delta g_{SF} \approx 4.55$) by the end of LC than an average vehicle performing CLC ($\Delta g_{SF} \approx 0.38$)). Note that at the start of the lane change, vehicles performing FLC had

TABLE 3. Summary of the comparative analysis of the ambient traffic state at the onset of two LC types.

EV	LC TYPE (sample size)	Mean (Std. Error)	Difference (Std. Error)	t	Sig (2-tailed)
g_{SF}(m)	CLC (762)	16.83 (0.48)	3.18	2.76	0.006
	FLC(263)	13.64 (1.04)	-1.02		
g_{LS}(m)	CLC (781)	12.37 (0.41)	-0.19	-0.22	0.819
	FLC(267)	12.54 (0.78)	-0.84		
g_{PS}(m)	CLC(647)	18.60 (0.45)	-2.3	-2.04	0.042
	FLC(184)	20.91 (1.03)	-1.13		
g_{LF}(m)	CLC(748)	28.90 (0.54)	2.39	1.78	0.075
	FLC(257)	26.51(1.22)	-1.34		
Δv_{SF}(m/s)	CLC (762)	-0.19 (0.09)	-0.99	-5	<0.001
	FLC(263)	0.79 (0.18)	-0.19		
Δv_{LS}(m/s)	CLC (781)	0.80 (0.09)	1.07	5.74	<0.001
	FLC(267)	-0.26 (0.17)	-0.19		
Δv_{PS}(m/s)	CLC(647)	-0.63 (0.08)	-0.09	-0.534	0.593
	FLC(184)	-0.54 (0.15)	-0.17		
Δv_{LF}(m/s)	CLC(748)	0.59 (0.07)	-0.1	-0.785	0.432
	FLC(257)	0.48 (0.11)	-0.13		

TABLE 4. Summary of the comparative analysis of the transition of ambient traffic state in each LC type.

EV	LC TYPE	Mean (Std error)	Difference (Std error)	t	Sig(2-tailed)
$[g_{SF}(t^{end}) - g_{SF}(t^{start})]$ in m	CLC (762)	0.38 (0.40)	-4.16	-4.05	<0.000
	FLC (263)	4.55 (0.94)	-0.88		
$[g_{LS}(t^{end}) - g_{LS}(t^{start})]$ in m	CLC (781)	-4.61 (2.05)	-3.75	-1.008	0.593
	FLC (267)	-0.85 (2.12)	-3.72		
$[\Delta v_{SF}(t^{end}) - \Delta v_{SF}(t^{start})]$ in m/s	CLC (762)	0.39 (0.09)	0.84	4.15	<0.001
	FLC (263)	-0.44 (0.19)	-0.2		
$[\Delta v_{LS}(t^{end}) - \Delta v_{LS}(t^{start})]$ in m/s	CLC (781)	-0.70 (0.09)	-1.14	-5.38	<0.001
	FLC (267)	0.43 (0.19)	-0.21		
$g_{SF}(t^{end}$ in m	CLC (762)	17.22 (0.33)	-0.97	-1.43	0.15
	FLC (263)	18.20 (0.60)	-0.69		
$\Delta v_{SF}(t^{end})$ in m/s	CLC (762)	0.20 (0.06)	-0.14	-1.17	0.24
	FLC (263)	0.34 (0.10)	-0.12		
$\Delta v_{LS}(t^{end})$ in m/s	CLC (781)	0.10 (0.06)	-0.06	-0.58	0.56
	FLC (267)	0.17 (0.09)	-0.11		

significantly shorter g_{SF} than vehicles performing a CLC (See Table 3).

Secondly, Table 4 shows that Δv_{SF} and Δv_{LS} exhibits a significantly different transition between the two LC's as shown in Figure 8. Table 3 shows that an average FLC (CLC) vehicle had higher (lower) velocity than the two vehicles in the target lane (See Figure 8). The results in Table 4 suggest that the speed difference was reduced during both types of LC's, and the transition was directed towards neutralising their initial values. Figure 8(a) and (b) show this trend clearly. More precisely, by the end of LC, an average FLC/CLC vehicle is at a smaller velocity difference with respect to F and L. In order to evaluate the role of each vehicle in the transition, let's first consider the interaction between S and L. In this interaction, L does not play an active role and therefore the transition is directly related to S. The respective transition of Δv_{LS} implies that an average FLC (CLC) vehicle reduces (increases) its relative velocity during lane change execution. This is consistent with the observation reported in Section III-A. that the vehicles performing an FLC (CLC) exhibit a negative (positive) value of average acceleration: -0.03 m/s^2 (0.05 m/s^2). Now let's consider the interaction between S and F, in which both the vehicles play an active role. The identified action of and the anticipatory behavior of F effect the transition of Δv_{SF}. More precisely, the reduction (increase) in velocity by an average FLC (CLC) vehicle and the anticipatory response of the F together reduce the speed difference between them. Figure 8(a) and (b) show this trend clearly. Therefore the results in Table 4 suggest that the FLC distinctly impact the follower in the target lane during LC. The mean g_{SF}, Δv_{SF} and Δv_{LS} are significantly different at the onset (See Table 3), but not at the end of LC (See
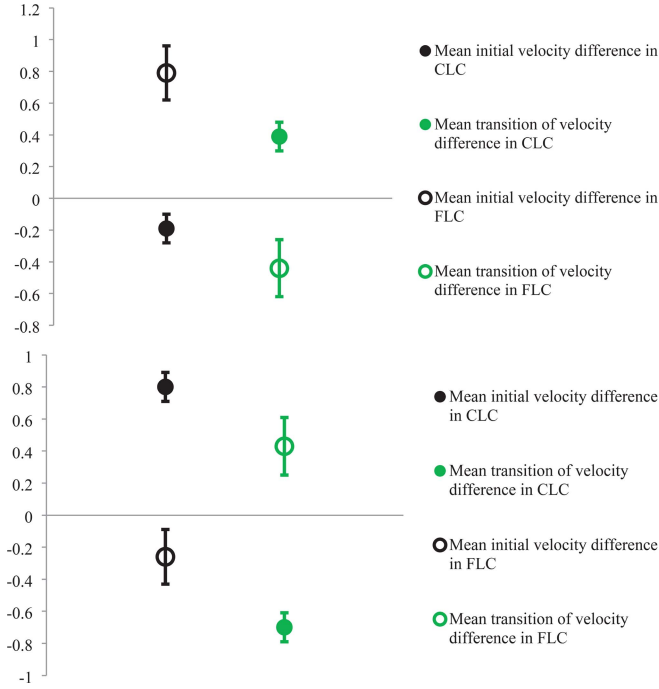
FIGURE 8. Estimates of initial and subsequent transition of the mean relative velocity: (a) Subject and Follower (b) Leader and Subject. In each figure, the velocity means are significantly different with p < 0.01.

FIGURE 9. Temporal evolution of average τ for all the followers during anticipation; τs are measured with respect to the lane-changers. On the x-axis, t = 0 s depicts the moment of lane change insertion.

Table 4). This suggests that both LC types ultimately results in similar local traffic conditions.

C. MODELS OF LC IMPACT ON THE TARGET-FOLLOWER

In the previous section, we identified that FLC induces a distinct transition on the follower in the target lane. The existing LC impact models describe the relaxation behavior and anticipation behavior, without differentiating the LC types. The relaxation process during the LC has been successfully modelled by [26]. This model was conceived from a microscopic car following model incorporating the macroscopic lane change model. Zheng *et al.* [16] showed that this model can describe the entire transition process: anticipation and relaxation. However, none of the existing models distinguishes the impacts of FLC and CLC. We revise the model in [16] to capture the entire transition process induced by specifically by the LC types. The transition model proposed by Zheng *et al.* [16] is built on the assumption that vehicles obey Newell's car-following model. This model provides the speed function of a vehicle corresponding to the triangular fundamental diagram. In this model, the trajectory of a vehicle i is identical to that of the preceding vehicle $i+1$ with a spatial shift d and a temporal shift τ. Thus d represents the minimum spacing and τ represents the time vehicle i waits until it responds (by manipulating its velocity) to a change in the velocity of the preceding vehicle $i+1$. The follower's transition process during a lane change is thereby modelled using a variation of its car-following parameter τ, i.e., this parameter temporarily deviates from the equilibrium value and gradually converges back. The formulation of the model
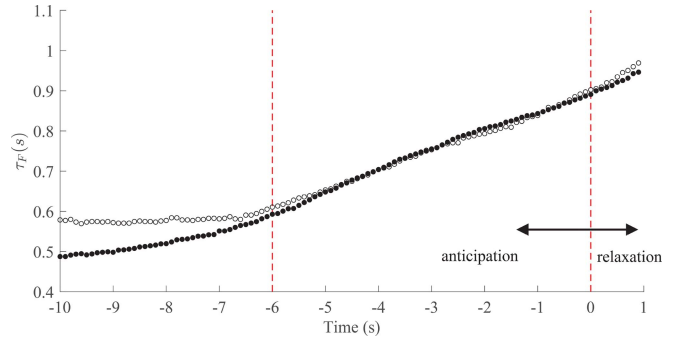
is as follows:

$$\tau^i(t) = \tau^i(0) + \frac{\varepsilon}{\beta} \ln\left(1 + \frac{\beta t}{w + v^{i+1}(0)}\right) \tag{5}$$

where $\tau^i(t)$ is the response time of the vehicle i at the time t, $\tau^i(0)$ is its initial response time at the start of the transition, ε is the speed difference that i is willing to accept, β is a constant acceleration rate of the lead vehicle $i+1$, w is the average velocity of kinematic waves and $v^{i+1}(0)$ is the initial speed of the vehicle $i+1$.

1) OBSERVING THE TRANSIENT BEHAVIOR OF THE TARGET-FOLLOWER

We measure the target-follower's response time τ as proposed by [16]. Here, τs are measured along the set of kinematic waves propagating backwards in space with a velocity w. The process starts with the lane-changer signalling the intention to change the lane at a time t_0^{i+1}, thereby emanating the first kinematic wave. The wave moves upstream and arrives at the vehicle i at the time t_0^i. Then τ along the first wave is computed as $t_0^i - t_0^{i+1}$.

As the results in Section IV-B show that FLC imposes a different impact on the follower in the target lane, we expect a difference in the anticipation process prior to FLC. To examine this, we filtered the pairs of lane-changers and immediate followers, those could be observed prior to the insertion, i.e., during $[t_{LC} - 10s, t_{LC} + 1s]$. A follower can be expected to exhibit the anticipation process only if its response time is shorter than the equilibrium car following response time (1.4 s). Hence, only the vehicle pairs with follower's $\tau < 1.4$ s during $[t_{LC} - 10s, t_{LC} - 5s]$ are included in the analysis. Accordingly, we identified 168 vehicle pairs involved in CLC's and 75 vehicle pairs involved in FLC's. Figure 9 shows the temporal evolution of τ observed during CLC's and FLC's. The insertion point t_{LC} is marked as t = 0 s, thereby separating the anticipation phase (t < 0) and the relaxation phase (t > 0). The insertion point t_{LC} has been considered to be a good approximation of the time instant when the follower switches from anticipation to relaxation [16]. During the anticipation phase, among the CLC samples, the average τ appears to be continuously
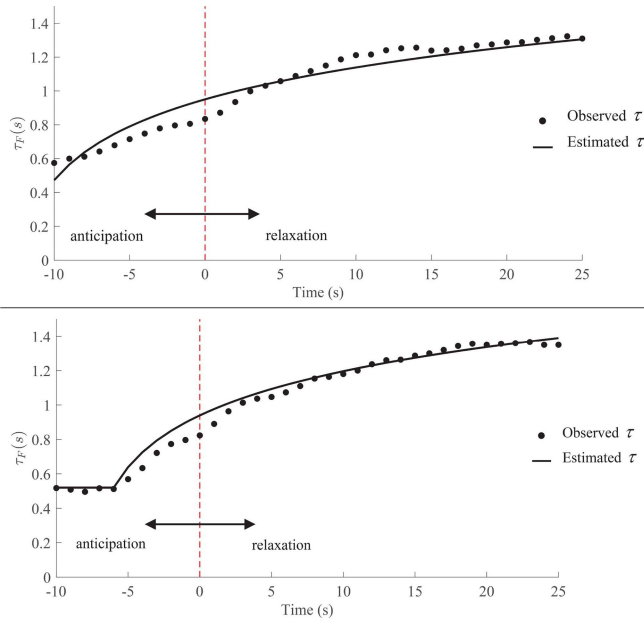
FIGURE 10. Temporal evolution of average τs for all followers (a) during continuous lane change; (b) during fragmented lane change.

TABLE 5. Summary of calibration results of the LC impact models.

	Model:CLC impact		Model:FLC impact	
	Mean	95% CI	Mean	95% CI
$\tau^i(0)$	0.472	(0.34,0.60)	0.52	(0.35,0.68)
ϵ	1.061	(0.63,1.48)	1.435	(0.95,1.91)
β	3.186	(1.18, 5.18)	4.441	(2.08,6.79)
RMSE	0.059		0.047	

increasing from −10 s. On the contrary, among the FLC samples, the evolution of average τ follows a different profile: it remains approximately constant for a finite time period initially (−10 s to −6 s). This could because the follower is not yet certain that the lane-changer would cut-in, and therefore maintains it's current τ. The response time is seen to steadily increase from −6 s, similar to the CLC. At the insertion time, followers (of both sets) exhibit a response time much below the equilibrium value ($\approx$ 1.4 s) and follow a similar trend. Figure 9 depicts the different anticipation profile of F when confronted with FLC: follower maintains a short for a finite time period, and thereafter increases τ to the equilibrium value.

To observe the entire transition process of the follower: anticipation and relaxation, the vehicles should be observed for a longer period, i.e., $T^+ \in [t_{LC} - 10s, t_{LC} + 25s]$ [14], [16]. A follower can be expected to exhibit the relaxation only if its response time deviates from the equilibrium value. As the equilibrium τ is approximately 1.4 s, only those followers with $\tau < 1$ s at $t - LC$ is considered in the analysis [14]. Additionally, the follower and lane-changer must not perform any other lane change than the one of our interests. This is to avoid the effects of multiple transition processes. Accordingly, we identified 52 vehicle pairs involving a CLC and 30 vehicle pairs involving an FLC. In order to capture the entire dynamic transition process, τs are measured along successive waves with an interval of 1 s, i.e., one out of ten τ samples is used for the modelling. This is consistent with the previous work by [16]. The temporal evolution of average of all followers is plotted in Figure 10(a) (for CLC samples) and 10(b) (for FLC samples). It can be seen that in both cases the followers attain a post relaxation equilibrium at around 15–17 s which is consistent with the study by [14].

2) MODEL CALIBRATION AND PERFORMANCE EVALUATION

As seen in the previous section, among the FLC samples, the mean value of τs did not exhibit an increasing trend during the initial phase of anticipation; instead, they remain approximately constant till 6 seconds prior to insertion. To capture this observation, we model the anticipation process of the follower in response to an FLC as $\tau^i(t) = \tau^i(0) : t \in [-10, -6]$. We adopt the same calibration procedure as in the previous studies on the same dataset [14], [16], and the use the same values of the parameter: $w = 5$ m/s and $v^{i+1}(0) = 5$ m/s. For each lane change sample, we simultaneously calibrate $\tau^i(0)$, ϵ and β by minimizing the root mean squared error between observed and predicted τ values of F with respect to the lane-changer. We used unconstrained optimisation with the Quasi-Newton algorithm for minimising the RMSE error. The mean parameter values and their 95% confidence intervals are detailed in Table 5. The RMSE value for the LC impact model of CLC is 0.059 and that of the FLC is 0.047, demonstrating good calibration performance. These results suggest that the follower undergo both anticipation and relaxation process irrespective of the lane change type it confronts. However, during the anticipation process for an FLC, the follower maintains its response time constant initially and increases thereafter.

To summarise, compared to CLC, FLC emerges under distinct traffic conditions. Moreover, FLC induces a distinct impact on the driving behavior of the follower in the target lane, particularly during the anticipation process. We show that this distinct response of follower to FLC can be captured by a simple extension of an existing model [16].

V. DISCUSSION

Compared to typical CLC's, this study revealed that FLC's represent a distinct type of lane change execution and induce a different impact on the ambient traffic. Additionally, we investigated the influence of lane change conditions and driver characteristics on the LC type.

Figure 11 depicts the percentage of FLC among total lane changes originating from every 100 meters of the study stretch. In the figure, Lane 6 is the rightmost lane and Lane 7 is the on-ramp lane that merges onto the motorway. It can be seen that the share of the FLC's increase up to 40 percent downstream of the merge on lanes 5, 6 and 7. In these locations, lane changes are typically performed either to merge onto the motorway or to move to the middle lane from the
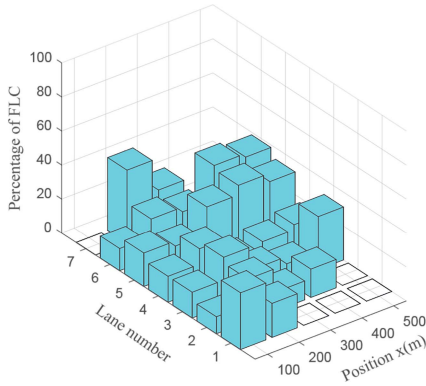
FIGURE 11. Percentage of fragmented lane changes among total lane changes per 100 meters in each lane.

FIGURE 12. Relationship between the characteristics of the follower and characteristics of the lane-changers (a) prior to the continuous lane change, (b) prior to the fragmented lane change.

rightmost lane [2]. This increased necessity to change lane might also explain why the driver performs FLC despite the lower velocity of the vehicle in the target lane as reported in Section IV-A.

We investigated if the characteristics of the driver such as being timid or aggressive influenced the choice LC type. The parameter has been used in several earlier studies to characterise driver behavior [16], [37]. We investigate the driver characteristics of the F and S prior to the lane change. The driver characteristic is represented by the deviation in τ at $t = -10$ s from the average $\bar{\tau}$ in $t \in [-10, -15]$. A driver is classified as timid if and as aggressive if $\tau > \bar{\tau}$ and as aggressive if $\tau < \bar{\tau}$. Figure 12 plots the characteristics of the follower against that of the subject prior to each type of lane change. Among the follower-subject pairs, we did not find a statistical difference in the distribution of driver aggressiveness between those involved in the two LC types.

The above two findings suggest that the choice of LC type in influenced by the necessity of lane change and not by the characteristics of the involved drivers. The findings and models cannot be generalized as they are derived from a single data set. The influence of infrastructure design and traffic state on the LC type, and prevalence of FLC among vehicle types other than cars are still unknown. A major challenge for research into FLC is the unavailability of empirical data records. Compared to CLC, FLC's are less frequent events and hardly observed in small data sets. Further efforts to observe and record the FLCs are necessary to model the process underlying the FLC decision and to yield generic insights.

VI. CONCLUSION

The study employs a rule-based algorithm to systematically identify and classify the lane-changing trajectory samples from NGSIM dataset. We find that FLCs constitute a considerable proportion ($\approx 30\%$) of lane changes, thereby confirming the finding by [24]. We show strong evidence that FLCs are performed by a distinct execution process. A vehicle moving along the FLC trajectory exhibits a statistically different lateral and longitudinal kinematics, and
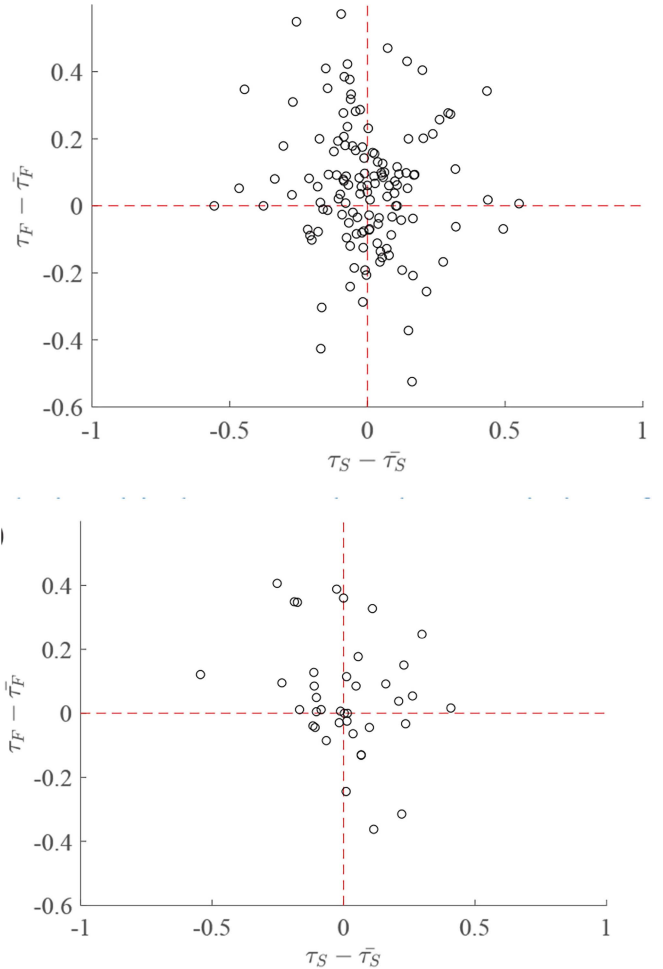
longer lane change duration (≈ 7.9 s). We propose a models to describe the kinematics and impacts of FLC which outperform other selected models.

Regarding the impact of FLC on the potential follower, we find that an FLC induces a distinct behavioral transition of the follower in the target lane, in terms of longitudinal kinematics. We find that a minor extension to the existing transition model by [16] with no additional parameters improves the accuracy of the LC impact model. Additionally, this study reveals that the ambient traffic state at the onset of FLC's is different from that of a CLC. Finally, our results suggest that a mandatory lane change condition is a factor motivating the driver to execute an FLC.

The insights and models presented in this the work have several applications. Traffic flow can be modelled more accurately by accounting for the distinct impacts and execution of FLC. Such a study can be performed with traffic flow simulation framework that depicts LC as a closed-loop process, such as the one proposed by Mullakkal-Babu *et al.* [38]. The results reinforce that the conventional representation of LC execution as an open-loop process is restrictive to

realistically model the LC and to describe maneuvers such as FLC. Future work will focus on the above-mentioned aspects.

REFERENCES

[1] L. Zheng, K. Ismail, and X. Meng, "Traffic conflict techniques for road safety analysis: Open questions and some insights," *Can. J. Civil Eng.*, vol. 41, no. 7, pp. 633–641, 2014.

[2] E. Balal, R. L. Cheu, and T. Sarkodie-Gyan, "A binary decision model for discretionary lane changing move based on fuzzy inference system," *Transp. Res. C, Emerg. Technol.*, vol. 67, pp. 47–61, Jun. 2016.

[3] M. Keyvan-Ekbatani, V. L. Knoop, and W. Daamen, "Categorization of the lane change decision process on freeways," *Transp. Res. C, Emerg. Technol.*, vol. 69, pp. 515–526, Aug. 2016.

[4] S. Moridpour, M. Sarvi, and G. Rose, "Modeling the lane-changing execution of multiclass vehicles under heavy traffic conditions," *Transp. Res. Rec. J. Transp. Res. Board*, vol. 2161, no. 1, pp. 11–19, 2010.

[5] M. Rahman, M. Chowdhury, Y. Xie, and Y. He, "Review of microscopic lane-changing models and future research opportunities," *IEEE Trans. Intell. Transp. Syst.*, vol. 14, no. 4, pp. 1942–1956, Dec. 2013.

[6] P. G. Gipps, "A model for the structure of lane-changing decisions," *Transp. Res. B, Methodol.*, vol. 20, no. 5, pp. 403–414, 1986.

[7] A. Kesting, M. Treiber, and D. Helbing, "General lane-changing model MOBIL for car-following models," *Transp. Res. Rec. J. Transp. Res. Board*, vol. 1999, no. 1, pp. 86–94, 2007.

[8] S. Moridpour, G. Rose, and M. Sarvi, "Modelling the heavy vehicle drivers' lane changing decision under heavy traffic conditions," *Road Transp. Res.*, vol. 18, no. 4, pp. 49–57, 2009.

[9] W. J. Schakel, V. L. Knoop, and B. van Arem, "Integrated lane change model with relaxation and synchronization," *Transp. Res. Rec. J. Transp. Res. Board*, vol. 2316, pp. 47–57, Jan. 2012.

[10] T. Toledo, H. N. Koutsopoulos, and M. Ben-Akiva, "Integrated driving behavior modeling," *Transp. Res. C, Emerg. Technol.*, vol. 15, no. 2, pp. 96–112, 2007.

[11] M. J. Cassidy and J. Rudjanakanoknad, "Increasing the capacity of an isolated merge by metering its on-ramp," *Transp. Res. B, Methodol.*, vol. 39, pp. 896–913, Dec. 2005.

[12] S. Ahn and M. J. Cassidy, "Freeway traffic oscillations and vehicle lane-change maneuvers," in *Proc. Transp. Traffic Theory*, 2007, pp. 691–710.

[13] Z. Zheng, S. Ahn, and C. M. Monsere, "Impact of traffic oscillations on freeway crash occurrences," *Accident Anal. Prevent.*, vol. 42, no. 2, pp. 626–636, 2010.

[14] A. Duret, S. Ahn, and C. Buisson, "Passing rates to measure relaxation and impact of lane-changing in congestion," *Comput.-Aided Civil Infrastruct. Eng.*, vol. 26, no. 4, pp. 285–297, 2011.

[15] L. Leclercq, N. Chiabaut, J. Laval, and C. Buisson, "Relaxation phenomenon after lane changing: Experimental validation with NGSIM data set," *Transp. Res. Rec. J. Transp. Res. Board*, vol. 1999, pp. 79–85, Jan. 2007.

[16] Z. Zheng, S. Ahn, D. Chen, and J. Laval, "The effects of lane-changing on the immediate follower: Anticipation, relaxation, and change in driver characteristics," *Transp. Res. C, Emerg. Technol.*, vol. 26, pp. 367–379, Jan. 2013.

[17] W. van Winsum, D. de Waard, and K. Brookhuis, "Lane change manoeuvres and safety margins," *Transp. Res. F, Traffic Psychol. Behav.*, vol. 2, no. 3, pp. 139–149, 1999.

[18] D. D. Salvucci and R. Gray, "A two-point visual control model of steering," *Perception*, vol. 33, no. 10, pp. 1233–1248, 2004.

[19] L. Li, C. Lv, D. Cao, and J. Zhang, "Retrieving common discretionary lane changing characteristics from trajectories," *IEEE Trans. Veh. Technol.*, vol. 67, no. 3, pp. 2014–2024, Mar. 2018.

[20] T. Toledo and D. Zohar, "Modeling Duration of Lane Changes," *Transp. Res. Rec. J. Transp. Res. Board*, vol. 1999, pp. 71–78, Jan. 2007.

[21] Q. I. Wang, Z. Li, and L. I. Li, "Investigation of discretionary lane-change characteristics using next-generation simulation data sets," *J. Intell. Transp. Syst.*, vol. 18, no. 3, pp. 246–253, 2014.

[22] S. Moridpour, M. Sarvi, and G. Rose, "Lane changing models: A critical review," *Transp. Lett.*, vol. 2, no. 3, pp. 157–173, 2010.

[23] D. Yang, L. Zhu, B. Ran, Y. Pu, and P. Hui, "Modeling and analysis of the lane-changing execution in longitudinal direction," *IEEE Trans. Intell. Transp. Syst.*, vol. 17, no. 10, pp. 2984–2992, Oct. 2016.

[24] D. Yang, L. Zhu, F. Yang, and Y. Pu, "Modeling and analysis of lateral driver behavior in lane-changing execution," *Transp. Res. Rec. J. Transp. Res. Board*, vol. 2490, no. 1, pp. 127–137, 2015.

[25] W. Yao, H. Zhao, F. Davoine, and H. Zha, "Learning lane change trajectories from on-road driving data," in *Proc. IEEE Intell. Veh. Symp.*, Alcala de Henares, Spain, 2012, pp. 885–890.

[26] J. Laval and L. Leclercq, "Microscopic modeling of the relaxation phenomenon using a macroscopic lane-changing model," *Transp. Res. B, Methodol.*, vol. 42, no. 6, pp. 511–522, 2008.

[27] A. Savitzky and M. J. Golay, "Smoothing and differentiation of data by simplified least square procedures," *Anal. Chem.*, vol. 36, no. 8, pp. 1627–1639, 1964.

[28] C. Thiemann, M. Treiber, and A. Kesting, "Estimating acceleration and lane-changing dynamics from next generation simulation trajectory data," *Transp. Res. Rec. J. Transp. Res. Board*, vol. 2088, pp. 90–101, Jan. 2008.

[29] R. Rajamani, "Lateral vehicle dynamics," in *Vehicle Dynamics and Control*, 2nd ed., F. F. Ling, Ed. Boston, MA, USA: Springer, 2012, ch. 2, pp. 12–46.

[30] P. Hofmann, G. Rinkenauer, and D. Gude, "Preparing lane changes while driving in a fixed-base simulator: Effects of advance information about direction and amplitude on reaction time and steering kinematics," *Transp. Res. F, Traffic Psychol. Behav.*, vol. 13, no. 4, pp. 255–268, 2010.

[31] D. Soudbakhsh, A. Eskandarian, and D. Chichka, "Vehicle collision avoidance maneuvers with limited lateral acceleration using optimal trajectory control," *J. Dyn. Syst. Meas. Control*, vol. 135, pp. 1–12, Jul. 2013.

[32] B. Zhou, Y. Wang, G. Yu, and X. Wu, "A lane-change trajectory model from drivers' vision view," *Transp. Res. C, Emerg. Technol.*, vol. 85, pp. 609–627, Dec. 2017.

[33] D. D. Salvucci and A. Liu, "The time course of a lane change: Driver control and eye-movement behavior," *Transp. Res. F, Traffic Psychol. Behav.*, vol. 5, no. 2, pp. 123–132, 2002.

[34] H. Jula, E. B. Kosmatopoulos, and P. A. Ioannou, "Collision avoidance analysis for lane changing and merging," *IEEE Trans. Veh. Technol.*, vol. 49, no. 6, pp. 2295–2308, Nov. 2000.

[35] J. Wang, J. Wu, and Y. Li, "The driving safety field based on driver—Vehicle—Road interactions," *IEEE Trans. Intell. Transp. Syst.*, vol. 16, no. 4, pp. 2203–2214, Aug. 2015.

[36] E. Balal, R. L. Cheu, T. Sarkodie-Gyan, and J. Miramontes, "Analysis of discretionary lane changing parameters on freeways," *Int. J. Transp. Sci. Technol.*, vol. 3, pp. 277–296, Sep. 2014.

[37] D. Chen, S. Ahn, J. Laval, and Z. Zheng, "On the periodicity of traffic oscillations and capacity drop: The role of driver characteristics," *Transp. Res. B, Methodol.*, vol. 59, pp. 117–136, Jan. 2014.

[38] F. A. Mullakkal-Babu, M. Wang, B. van Arem, B. Shyrokau, and R. Happee, "A hybrid submicroscopic-microscopic traffic flow simulation framework," *IEEE Trans. Intell. Transp. Syst.*, early access, May 6, 2020, doi: 10.1109/TITS.2020.2990376.

FREDDY ANTONY MULLAKKAL-BABU received the master's degree in transportation systems engineering from the Indian Institute of Technology, Mumbai, and the Ph.D. degree in transport and planning from the Delft University of Technology, the Netherlands, in 2014 and 2020, respectively. Since 2019, he has been working as a Simulation Engineer with Siemens PLM Software. His main research interests include driver behavior modeling, traffic safety and design, and assessment of driving automation systems.

MENG WANG (Member, IEEE) received the M.Sc. degree in transportation engineering from the Research Institute of Highway, China, and the Ph.D. degree in transport and planning from the Delft University of Technology, the Netherlands, in 2006 and 2014, respectively. From 2014 to 2015, he was a Postdoctoral Researcher with the Department of Biomechanical Engineering, Delft University of Technology, where he has been an Assistant Professor with the Department of Transport and Planning, since 2015. His main research interests include driving behavior modeling, traffic flow, and control approaches for cooperative driving systems.

RIENDER HAPPEE received the M.Sc. degree in mechanical engineering and the Ph.D. degree from the Delft University of Technology, the Netherlands, in 1986 and 1992, respectively. He investigated road safety and introduced biomechanical human models for impact and comfort with TNO Automotive from 1992 to 2007. He currently investigates the human interaction with automated vehicles focussing on safety, comfort and acceptance with the Delft University of Technology, the Netherlands, where he is an Associate Professor with the Faculties of Mechanical, Maritime and Materials Engineering, and Civil Engineering and Geosciences.

BART VAN AREM (Senior Member, IEEE) received the master's degree in 1986 and the Ph.D. degree in applied mathematics, with a specialty in queuing theory from the University of Twente, the Netherlands, in 1990. He was a Researcher and a Program Manager with TNO from 1992 to 2009 on intelligent transport systems, where he was involved in various national and international projects. Since 2009, he has been a Full Professor with the Department of Transport and Planning, Delft University of Technology, with a focus on the impact of intelligent transport systems on mobility. His research interest focus on advanced driver assistance systems.